



UNIVERSITY OF AMSTERDAM
SYSTEM & NETWORK ENGINEERING

Research Project 1

Ranking of manipulated images in a large set using Error Level Analysis

Authors:

Daan Wagenaar
daan.wagenaar@os3.nl

Coordinators:

Zeno Geraads
zeno@holmes.nl

Jeffrey Bosma
jeffrey.bosma@os3.nl

Marcel Worring
m.worring@uva.nl

Abstract

In this paper, we propose several methods for ranking a set of images based on the likelihood of being manipulated. All of these ranking methods utilize the Error Level Analysis (ELA) algorithm to yield a qualifier for each image which is then used to rank images with a high probability of image manipulation on top. By doing so, we hope to reduce the amount of work an expert needs to verify the authenticity of the images in such a set. In our experimental setup, a set of 300 images was created using three digital cameras from different brands (Canon, iPhone, Samsung). A third-party performed copy & move image manipulations on 30 randomly selected images in this set. Each developed ranking method is run at an ELA quality level of 75%, 85%, and 95%. The gathered results show the best rankings for our methods at an ELA quality level of 95%. However, many false-positives, both authentic and manipulated images, make the final ranking not suitable as an alternative to an exhaustive search in which each image is checked manually by an expert.

February 13, 2012

Contents

1	Introduction	1
1.1	Image Manipulation	1
1.2	Manipulation Detection	3
1.3	Related Work	3
1.4	Research Question	5
2	Theory	6
2.1	Image Representation	6
2.2	Image Compression	7
2.2.1	Lossless Compression	7
2.2.2	Lossy Compression	7
2.3	JPEG Image Format	7
2.4	Error Level Analysis	8
2.4.1	Limitations	10
3	Methodology	11
3.1	Method 1: Average RGB values per block	11
3.2	Method 2: Block to block comparison	12
3.3	Method 3: Colored pixels ratio	12
3.4	Method 4: Highest luminance value of the brightest pixel	12
3.5	Method 5: Average luminance value of the 64 brightest pixels	12
3.6	Method 6: Average luminance value of the brightest block	13
4	Experiments	14
4.1	Proof of Concept	14
4.2	Experiments	14
4.2.1	Goal	14
4.2.2	Setup	14
4.2.3	Evaluation Criteria	15
5	Results	16
6	Discussion	18
7	Conclusion	24
8	Further Research	25
Acronyms		26
Acknowledgements		27
Bibliography		29
A	Overview of Performed Manipulations	30
B	Overview of Manipulated Images	31
C	Highest 10 Ranking Results	43
D	Lowest 10 Ranking Results	45
E	Ranking of Internal Copy & Move Manipulated Images	47

Chapter 1

Introduction

Digital images play an ever more important role in today's modern society. Digital cameras are widely available to the general public and with the rise of the current generation, camera integrated, smartphones, images can be shot, edited and shared in a matter of seconds.

With image shooting and editing capabilities at a person's fingertips, it is sometimes questionable whether or not images are real. In cases where images are purely used for entertainment purposes, this is not considered a very big issue. However, in cases where images become evidence, it is ever more important to be able to verify the authenticity and integrity of these images.

Commonly, images are checked for manipulation by an expert that visually inspects them. This is not a problem when only a small set of images need to be confirmed as usable evidence. However, doing the same for a large sets of images quickly becomes a tedious and time consuming process. Our research focuses on the ranking of large sets of images based on the likelihood of being manipulated, as well as the effectiveness and reliability of using such a ranking method.

1.1 Image Manipulation

Many different image manipulation techniques exist today. For instance, a person might want to remove the red-eye effect [1] in an image from pupils that have a red glow. or enhance the image's brightness to improve the appearance of the subject. The most common forms of image manipulation are the so called 'copy & move' manipulations [2], [3], and usually entail one of the following techniques:

- Removing an object from an image.
- Changing the appearance of an object in an image.
- Adding a foreign object to an image.

For each of these manipulation techniques, a distinction is made between so called internal and external copy & move image manipulation. With internal copy & move manipulations, an object is copied and moved within the image that is being manipulated. In the other case, with external copy & move manipulations, an object is copied from another image (external source) and moved into the image that is being manipulated.

Figure 1.1 and 1.2 illustrate an example of where an object is removed from the original image and is no longer present in the manipulated image. In figure 1.1, the original image is illustrated where Stalin's commissar of water transport, named Nikolai Yezhov, is clearly present. However, in the manipulated image illustrated in figure 1.2, Nikolai has been removed completely without leaving any visible traces (to the untrained eye). In this case, an internal copy & move manipulation was performed.



Figure 1.1: Original image [4]



Figure 1.2: Stalin without Yezhov [4]

Figure 1.3 illustrates an original image taken of Katie Couric during a marketing campaign in 2006. Figure 1.4 illustrates the manipulated image in which the body of Katie has been slimmed down, essentially changing her appearance. Again, this case is an example of internal copy & move manipulation.



Figure 1.3: Original image [5]



Figure 1.4: Slimmed down Katie Couric [5]

Lastly, figure 1.5 illustrates an original image of two students of the University of Amsterdam. The image in figure 1.6 was manipulated and illustrates the addition of a foreign object, namely a white-colored mobile phone that was not part of the original image. Since the mobile phone did not come from the original image itself, an external copy & move manipulation was performed.

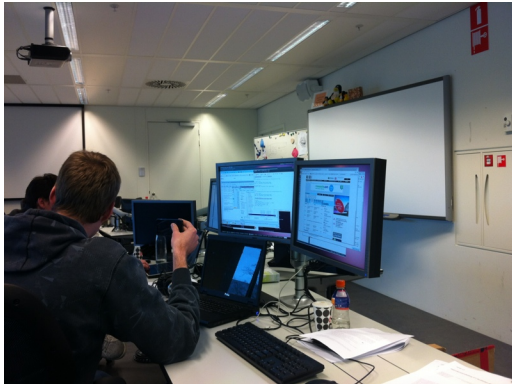


Figure 1.5: Original image



Figure 1.6: Added white mobile phone

1.2 Manipulation Detection

Not only are there techniques for manipulating images, fortunately there also are techniques for detecting manipulation.

Images are stored in different image formats such as Joint Photographic Experts Group (JPEG), Graphics Interchange Format (GIF) [6], Portable Network Graphics (PNG) [7], Tagged Image File Format (TIFF) [8], and RAW [9]. Besides the data that is part of the visible content of an image, these image formats also contain all sorts of additional data called metadata. A popular metadata format used for images is the Exchangeable Image File Format (EXIF) [10]. In most cases the image's associated metadata can be as useful as the image itself. The metadata of an image contains essential information such as its dimensions, but usually also other nonobligatory information such as the brand and model of the camera that took the image, the date and time when being shot, and the colorspace that was used. Some image manipulation software changes, for instance, the information about the camera model to the name of the program [11]. Looking for these kind of discrepancies is called image format analysis [12] and is considered an active approach of detecting image manipulation [13].

However, image format analysis does not evaluate the image itself but only its metadata. Techniques such as Luminance Gradient (LG), Principal Component Analysis (PCA), Wavelet Transformations (WT), and Error Level Analysis (ELA), all explained in section 1.3, allow for the identification of specific image manipulations [12]. These techniques are considered being a passive approach of image manipulation detection and require no prior information about the investigated image or its source [13]. In the case of the mentioned techniques, the results are visualized into another image that contains technique-specific highlighting. The highlighting in such a visualization is used by an expert to analyze the questionable image on its authenticity and integrity.

1.3 Related Work

As said, there exist different image manipulation detection techniques, such as the four mentioned in section 1.2. Although these four techniques are all related in the sense that they share a common purpose, namely aiding in the detection of image manipulation, there is a completely different theory underlying each of them. For each of these techniques, in the order LG, PCA, WT, and ELA, respectively, some key aspects will be explained.

Luminance Gradient

LG is used to identify manipulation of an image by illustrating the general direction of light. To do so, LG utilizes the fact that light rarely hits an object with an uniform intensity. Instead, sections of an object that are closer to the light source will appear brighter. There are many variations of LG, however, they all aim to identify the light direction.

In the simplest variation, the image is divided into squared blocks of a fixed size, e.g. 3 by 3 pixels. For every block the direction of light is identified based on adjacent pixels in the block that appear brighter in a certain direction. This is done for every block which results in a set of directions, one direction per block pointing towards the brightest local light source. Finally, the color of every block is remapped based on the direction of the local light source. For example, a direction pointing to the right means all green, to the left means no green, upwards means all red, and downwards means no red. This results in another image that is then used by an expert to determine if the image was manipulated based on the transition of different colored surfaces. Smooth surfaces with even gradient transitions or no transition at all suggest digital manipulation or computer graphics [12].

Principal Component Analysis

PCA is used to identify the color spectrum within an image. PCA finds patterns in the image data and expresses this pattern data in a certain way to highlight their similarities and differences [14]. Assume an entire image is plotted in three dimensions based on the colors of the pixels: red is mapped to the X-axis, green is mapped to the Y-axis, and blue is mapped to the Z-axis. The resulting plot for most images has a narrow range of colors that appear as a large cluster. Since the image's plot is three-dimensional, there are three Principal Components (PCs). Each PC defines a plane across the plot and emphasizes different sections of information. PC1 identifies the widest variance across the color set, PC2 the second widest variance with respect to PC1, and PC3 the smallest variance.

For example, when areas of two different images and color sets are spliced together, they usually end up forming two distinct clusters. With PCA, areas within the image that come from different clusters will have noticeably different values.

In the end, PCA is used to detect image manipulation by rendering the distance from each pixel to a PC in another image. Each different PC that is used for rendering will yield a different image that is further analyzed by an expert [12].

Wavelet Transformations

WT utilizes the properties of wavelets to identify image manipulation. A wavelet is a specific function which is used to analyze signals. Any signal can be decomposed into a set of wavelets that, when combined, give an approximation of the signal. Approximating a signal with wavelets is actually also a form of compression. With images, the image is the signal and all wavelets together approximate this image. To be able to perfectly recreate the image, the total amount of wavelets that are required is equal to the amount of pixels in the image per color channel. Even if only a small percentage of the wavelets are used to render the image, the objects in the image are recognizable even though they are blurry. Using a higher percentage of wavelets causes the image to sharpen up and coloring to increase. Ultimately the entire image should sharpen at the same rate. WT uses this property to aid image manipulation detection. If areas of the image are manipulated by scaling or merging, i.e. using different layers in an image editor, then these areas will sharpen at different rates [12].

Error Level Analysis

ELA is used to identify image manipulation by detecting areas in an image that have a different level of compression error compared to a given level. Essential is that ELA makes use of the properties of image formats that utilize lossy compression. Just like the other image manipulation detection techniques explained earlier, applying ELA to an image results in a visual output in the form of a new image with dimensions equal to the processed image. In this newly generated image, manipulated areas with a different level of compression error stand out because they are visually contrasting in comparison to unmodified areas. An expert analyzes this image to determine if the processed image is authentic.

The above image manipulation detection techniques all have their merits and disadvantages. For our research, ELA forms the basis of the ranking process ELA is the most appropriate because its results are more distinctive and allow for easier interpretation than those provided by the other three techniques. Therefore, by analyzing the results generated by ELA we have a greater chance of succeeding. The theory that underlies ELA is explained in chapter 2.

1.4 Research Question

As explained, the results produced by ELA still need visual confirmation by an expert, which is a tedious and long process when a large set of images needs to be checked. With our research we aim to find a way to use ELA on a set of images, ranking each image based on the likelihood of being manipulated. By doing so, one could potentially limit the amount of manual interaction needed to confirm image manipulation.

Ultimately, the above leads to the following research question:

- Can the Error Level Analysis technique be used to rank a set of images according to potentially present image manipulation?

Although ELA works on different image formats that utilize lossy compression, the research is limited to the JPEG image format since it is among one of the most popular image formats in imaging applications ranging from Internet to digital photography [15]. Nevertheless, the research results should in theory also apply to images in other image formats that utilize lossy compression.

Chapter 2

Theory

Our research is based on several theoretical aspects such as image representation, image compression, the JPEG image format and the ELA technique. Since the theory of these aspects are fundamental, and will be heavily depended upon by the successive chapters, they are explained below.

2.1 Image Representation

Most information in this section comes from [16] which gives an easy to understand introduction to image representation.

Images are composed of a large amount of discrete units known as pixels. A pixel essentially is nothing more than a single square, a rectangular region to be precise, set to one specific numerical color value. The amount of horizontal and vertical pixels in an image determine respectively its horizontal and vertical dimension, better known as resolution. The more pixels an image is composed of, thus the higher the resolution, the smoother shapes in the image become since the density of the pixels increases.

To specify a location for each individual pixel, a graphics format is needed. The bitmap graphics format, also known as raster graphics format, is used by the JPEG image format to map a pixel to a certain location in an image.

A color model is required to translate between the color values of pixels and the actual colors that correspond to those values. The possible colors that can be represented by a color model is defined by a so called colorspace, and determined by the sample precision in bits (1 bit allows for black-and-white, 2 bits allows for 4 colors, et cetera). The most commonly used color model in computer applications is known as RGB, which is short for Red, Green, and Blue. JPEG images however are almost always stored using another color model known as YCbCr. The intensity of an image, referred to as luminance, is expressed by the letter Y. The letters Cb and Cr are referred to as chrominance and specify the blueness and redness of an image, respectively. Unlike the RGB color model, where all three components are roughly equal, the YCbCr color model concentrates the most important information in the Y component. Doing so allows for an increase in compression of JPEG images by including more data from the Y component than from the Cb and Cr components.

As mentioned above, JPEG uses the bitmap graphic format. The main drawback of this type of graphic format is that the storage space that is required to store the image, rapidly grows as the image resolution and colorspace increases. As explained in section 2.2, the solution is to apply compression to the data making up the image.

2.2 Image Compression

At the bit-level, an image can be seen as a set of data. The general idea behind compression is to mathematically reduce the amount of information needed to represent an identical or similar set of data that makes up an image. This is done by exploiting certain patterns in a set of data. When compression is applied on such a set, the storing and transferring of this set is more efficient in comparison to an uncompressed set. Performing compression requires computing power to do the actual work of reducing the stored information that is needed. In turn, compressed data must be decompressed first in order for it to be useful again.

There are two types of compression algorithms: lossless and lossy.

2.2.1 Lossless Compression

Algorithms for lossless compression reduce the total amount of information needed to store an image without losing any of the original image quality. In other words, the original value of every single bit before compression is preserved after decompression. The downside is that lossless compression does not reduce the file size as much as lossy compression would. Lossless compression algorithms are often used when image quality is more important than file size.

2.2.2 Lossy Compression

Lossy compression algorithms make use of the limitations of the human eye, such as having a hard time to distinguish between nearly identical colors [16]. Some information can be discarded without losing much of the original visual structure. The compression levels in most lossy compression algorithms can be adjusted and as these increase, the file size is reduced, sacrificing image quality due to image degradation. At the highest compression levels, image deterioration becomes more prominent, causing compression artifacts [17].

2.3 JPEG Image Format

Image files in the JPEG image format carry either the 'JPG' or the 'JPEG' file extension. JPEG is an image format that utilizes a compression algorithm. In all cases described in this research report, JPEG is used as a lossy image format. A detailed description of how the JPEG compression algorithm works is beyond the scope of this document. However, in short, the compression algorithm essentially consists of the five steps listed below. For a more detailed description of JPEG you are advised to read [18].

1. Divide the image in blocks of 8 by 8 pixels:

The first step of the compression algorithm is to divide the entire image into blocks of 8 by 8 pixels. Each block is then further processed without any relation to the other blocks.

2. Transform the RGB color space to the YCbCr color space:

Each pixel within a block is represented by RGB values and is called an RGB vector. The values in an RGB vector usually have significant amount of correlation and therefore need to be converted to something that has less correlation. This is done for better compression results.

3. Apply Discrete Cosine Transformation (DCT):

The heart of the JPEG compression algorithm is the Discrete Cosine Transformation. Basically, DCT transforms each block into a so called coefficient which can later be used in the process to decompress the image. DCT relies on the premise that pixels in an image exhibit a certain level of correlation with their neighboring pixels. Consequently, these correlations can be exploited to predict the value of a pixel from its respective neighbors [19].

4. Apply quantization:

The coefficients from the DCT process are stored as integers. Since integers are natural numbers, the coefficients need to be rounded before they can be saved. This is where the quantization comes in. The quantization process is the actual part of the compression algorithm that makes it a lossy compression algorithm since rounding the coefficients to integers will lead to losing some of the original data.

5. Apply Huffman encoding:

The last step in the compression algorithm is to encode the transformed and quantized image. For this purpose, the Huffman encoding technique is used. The idea behind Huffman coding is to identify pixels that occur frequently in an image and assign them short bit representations. Pixels that occur infrequently in an image are assigned long bit representations. Doing so will result in less data needed to be stored.

Some more aspects of the JPEG image format are explained in section 2.4 as part of the theory that underlies ELA.

2.4 Error Level Analysis

As mentioned in section 2.3, JPEG utilizes lossy compression. This means that if an image is saved using the JPEG image format, some information is lost due to quantization. The losing of information introduces what is known as error. The amount of information that is lost and the amount of error that is gained, is determined by the level of quality the JPEG image is saved at. JPEG quality levels are expressed in percent by values ranging from 0 up to 100. The basic rule here is that the higher the numerical value of the quality level, the less information is lost.

Furthermore, resaving a JPEG image will impact the quality of the image, even though no changes were made. For example, if an image initially compressed at a quality of 90% is resaved at a quality of 90%, the result is equivalent to a one-time save at 81%. This is calculated by taking 90% of 90%, essentially meaning the n^{th} resave at 90% should be approximately equivalent to $90\%^n$ [12], [20]. Another example is where an image at an initial quality of 75% is resaved at a quality of 90%, then the resulting image will have a quality of 67.5%.

It is interesting to note that the amount of information that is lost by each resave is not linear, as illustrated by the curved line in figure 2.1. The figure illustrates what happens to the quality of an image initially compressed at 75% when it is resaved ten times at a quality of 75%.

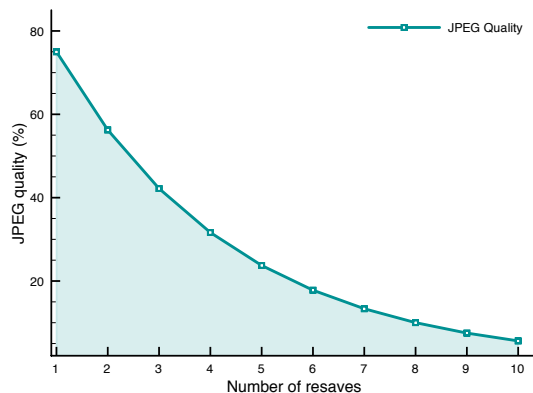


Figure 2.1: JPEG quality after resaving

The amount of error introduced by each save, is limited to the 8 by 8 blocks used by the compression algorithm of JPEG. However, when an image is (partially) modified, the 8 by 8 blocks containing modification are no longer at the same level of quality as the rest of the unmodified blocks.

The way ELA works is by resaving a potentially manipulated image at a certain given quality level, e.g. 95%. Doing so intentionally introduces a known error rate. Each 8 by 8 block at the same location in both images, namely the potentially manipulated image and the resaved image, are compared and the error state difference between the two is calculated. According to [12], if there is little to no difference, this indicates that the block in the resaved image has reached its minimal error state at the given quality level (in this example 95%). However, if there is a substantial amount of difference, then the block is not at its minimal error state. This information is translated into another image, which as said has a resolution identical to the potentially manipulated image, where for each block the amount of difference in error is visibly expressed by different levels of brightness. The closer the given quality level is to that of a block, the smaller the difference will get and the darker this block will appear in the output image. To illustrate this, a few examples follow.

Figure 2.2 illustrates an original image at a quality of 96%. Figures 2.3, 2.4 and 2.5 illustrate the ELA output images at a quality of 75%, 85%, and 95%, respectively. In figure 2.5, ELA indicates that the difference in error for all blocks is very small.



Figure 2.2: Original image



Figure 2.3: Result of ELA at 75%



Figure 2.4: Result of ELA at 85%



Figure 2.5: Result of ELA at 95%

Figure 2.6 illustrates the same image as seen in figure 2.2, with the exception of an image manipulation technique that was used: an external copy & move manipulation was done to add a tree to the image. In ELA, figures 2.7, 2.8, and 2.9 illustrate the difference in the brightness between the original and manipulated areas of the image. These differences make the manipulated areas stand out because they are visually contrasting in comparison to original areas. Furthermore, the figures illustrate, as to be expected, that different quality levels used for ELA severely impact the overall brightness of the output image, including that of the manipulated areas.



Figure 2.6: Original image



Figure 2.7: Result of ELA at 75%



Figure 2.8: Result of ELA at 85%

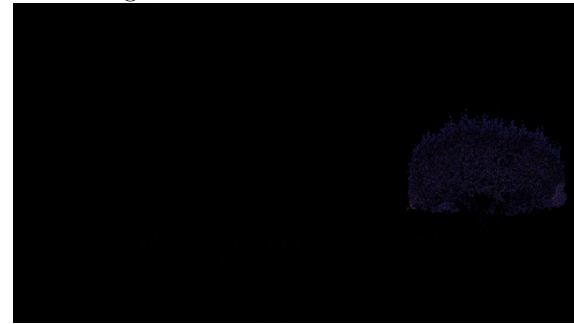


Figure 2.9: Result of ELA at 95%

2.4.1 Limitations

Although ELA does a fairly good job at visually outlining areas that are manipulated, the results differ per image. According to [12] and [20], ELA cannot be applied to all images and the results may not be conclusive, but are good enough for most images. The correctness of the results depend on the characteristics of the image that is being analyzed. For one, it is possible that because of the ELA results, authentic images are incorrectly identified as being manipulated. Also, it could also happen that based on the results of ELA, one is unable to distinguish areas that have been manipulated from areas that are authentic. Both of these different types of limitations are separated into two categories: false positives, authentic images that are detected as being manipulated, and false negatives, manipulated images that are not detected as being manipulated. For each category, a listing below contains some of the limitation.

False positives can be caused by:

- an image with a sharp contrast, well-defined patterns;
- an image with (a significant amount of) recoloring, such as brightening, pallet skew, et cetera [12].

False negatives can be caused by:

- an image that is very small;
- an image that has been scaled;
- an image with a low quality, either due to a very low JPEG quality setting or from color reduction;
- an image that has been scanned in, i.e. from a photo, magazine, or TV signal;
- an image that has been manipulated or computer generated by a skilled artist with an extreme level of talent [12].

Chapter 3

Methodology

Verifying the authenticity of a large set of images can be cumbersome and time consuming. Therefore we propose several methods that can help in identifying potentially manipulated images in a ranking order. A individual qualifier for each image in the set will be calculated and used in the final ranking process.

Each image in the set of images suspected to contain manipulated images, is initially processed by ELA. The resulting image, as explained in section 2.4, will be used and interpreted by the proposed methods.

Images consist of a total set of pixels P with each individual pixel $p \in P$. Each p consists out of RGB channel values R, G, B , or in short, RGB values.

Blocks of 8 by 8 pixels are defined for the methods that require the usage of blocks. The size of the blocks is exactly the same as used in the compression algorithm of JPEG. By doing so, we can be sure that the blocks used in the methods have the corresponding luminance values for the error introduced into a block by the JPEG compression algorithm. The total set of blocks per image is defined as B with each individual block $b \in B$. Each individual block b consists of a set of 64 pixels $N = \{I_1^b, I_2^b, I_3^b, \dots, I_{62}^b, I_{63}^b, I_{64}^b\}$ where I is a pixel of b and $n \in N$.

The luminance value of a pixel can be calculated from the RGB channel values by using a formula that represents how strong the human eye perceives brightness for certain colors. This theory is explained in [21]. We can obtain the luminance value L from the RGB channel values for each $p \in P$ by calculating $0.299 * R_p + 0.587 * G_p + 0.114 * B_p$.

3.1 Method 1: Average RGB values per block

Section 2.4 explains that manipulated areas are perceived brighter compared to authentic areas. By assuming that the RGB values in these areas are higher compared to areas where there is no manipulation, we can say that the higher the RGB values, the more likely a manipulated area is present. Taking the highest calculated RGB values for each image, we can built a ranking where the higher the RGB values, the higher the image is ranked.

Each image is split in blocks. The total value of the RGB channels for each pixel in each block is calculated. The highest average RGB values amongst the blocks is used as the qualifier. Formula 3.1 is the corresponding expression.

$$qualifier_1 = 1/64 \max_{b \in B} \left(\sum_{n \in N}^{#N} R_n^b + G_n^b + B_n^b \right) \quad (3.1)$$

The perceived brightness by the human eye, as stated in [22], is mainly influenced by the type of color. Green being perceived as the brightest color and blue as the least brightest color. The assumption that the higher the cumulative RGB channel values, the higher the brightness, is incorrect and may therefore lead to incorrect ranking of the images.

3.2 Method 2: Block to block comparison

Pixels in manipulated areas appear not only brighter, but are also clustered as illustrated in figures 2.7, 2.8, and 2.9. Therefore, if the image is divided into blocks, there should be a relatively low difference between the perceived brightness between blocks in authentic images, but a large difference between the perceived brightness between blocks in manipulated images.

Each image is split in blocks. For each block, the total value of the RGB channels for each pixel is calculated. The total RGB values for each block is than compared to the cumulative RGB channel values for all the remaining blocks X with $x \in X$. A representation can be seen in equation 3.2.

$$qualifier_2 = \max_{b \in B, x \in X} \left(\sum_{n \in N}^{#N} R_n^b + G_n^b + B_n^b - \sum_{n \in N}^{#N} R_n^x + G_n^x + B_n^x \right) \quad (3.2)$$

Figures 2.7, 2.8, and 2.9 illustrate that large parts of the image are black. The cumulative RGB channel values for a block in a black area is zero. This will always result in the difference being the value of the block it is compared against. Therefore, this method essentially results in using the same qualifier as method 1.

3.3 Method 3: Colored pixels ratio

In section 2.4 it is explained that performing ELA with a JPEG quality level of 95% yields a result with hardly any colored pixels. However, images that contain manipulated areas show significantly more colored pixels than authentic images as illustrated in figures 2.2 to 2.5 and 2.6 to 2.9.

For each image we extract all the black pixels P_{black} from the total amount of pixels P_{total} . This results in the number of pixels that make up the noise which in turn is used as the qualifier. Formula 3.3 shows the corresponding expression.

$$qualifier_3 = (P_{total} - P_{black})/P_{total} \quad (3.3)$$

3.4 Method 4: Highest luminance value of the brightest pixel

The same principle, namely that manipulated areas are brighter than other areas, mentioned in method 1, is applicable in this method. For each pixel, the luminance value is calculated. Finally, the luminance value of the brightest pixel is used as the qualifier. Formula 3.4 is the corresponding expression.

$$qualifier_4 = \max_{p \in P} (0.299 * R_p + 0.587 * G_p + 0.114 * B_p) \quad (3.4)$$

3.5 Method 5: Average luminance value of the 64 brightest pixels

To reduce the risk of outliers influencing the qualifier, additions to method 4 have been developed. The assumption is made that pixels forming the manipulation are clustered but not necessarily in the same block, if the image would be split in blocks. By taking the same amount of pixels of a 8 by 8 block, 64 pixels, a more accurate qualifier can be calculated.

For each pixel, the luminance value is calculated. The set σ contains the, by luminance value, ordered set of the top 64 pixels. The final qualifier is the average value of the ordered set σ . The corresponding expression can be seen in 3.5

$$\begin{aligned}
\forall p \in Pf : & 0.299 * R_p + 0.587 * G_p + 0.114 * B_p \\
& \sigma(L_{p_1}, L_{p_2}, L_{p_3}, \dots, L_{p_{62}}, L_{p_{63}}, L_{p_{64}}) \\
& \textit{qualifier}_5 = 1/64 \sum_{i \in \sigma}^{#\sigma} i
\end{aligned} \tag{3.5}$$

3.6 Method 6: Average luminance value of the brightest block

When disregarding the assumption made in section 3.5, using blocks instead of pixels could potentially allow for a more stable result. By splitting the image into blocks and calculating the average luminance value for that block, outliers are accounted for and clusters of bright pixels result in blocks with higher luminance values.

The average luminance value for the brightest block is calculated by taking the sum of the luminance value of each pixel in the block, divided by the number of pixels present in the block. Figure 3.6 shows the formula for calculating the qualifier.

$$\textit{qualifier}_6 = 1/64 \max_{b \in B} \left(\sum_{n \in N}^{#\mathcal{N}} 0.299 * R_n^b + 0.587 * G_n^b + 0.114 * B_n^b \right) \tag{3.6}$$

Chapter 4

Experiments

4.1 Proof of Concept

The in chapter 3 discussed methods 3, 4, 5, and 6 are implemented in a proof of concept. As said, these four methods are chosen as they prove to be the most usable.

4.2 Experiments

4.2.1 Goal

The goal of the experiment is to obtain a ranking of a set of images with manipulated images being ranked high in the list, ultimately testing the theory behind the ranking methods that were designed, as well as their effectiveness and reliability.

4.2.2 Setup

For the experiment, a total of 300 images are used. They are shot with three different digital cameras, to make sure the final results are not camera dependent, using the highest available resolution and quality setting (effectively the lowest available JPEG compression). Moreover, by doing so images are ensured to be authentic and not to have been tampered with. The three following digital cameras are used:

- Canon PowerShot A630
- iPhone 4
- Samsung Digimax S500

These cameras are chosen because they are available at hand, other than that there is no reason as to why these particular brands and models are used.

The first hundred images will be shot with the Canon PowerShot A630, the second hundred images with the iPhone 4, and the final hundred images with the Samsung Digimax S500. Of these 300 images, 30 images are randomly selected by a third-party for manipulation. The alterations done by the third-party consist out of different copy & move manipulations. The third-party will choose its own techniques to apply the manipulations and will keep this information classified up until the gathered results are analyzed. After completing the experiment, the third-party will disclose the information about the images that were manipulated along with a description of the manipulations done.

The experiment will be performed at three different ELA quality levels: 75%, 85%, and 95%.

4.2.3 Evaluation Criteria

The outcome of the experiment will be a comparison of the different ranking methods. In this comparison the best method is determined based on the following evaluation criteria:

- the effectiveness of the method in ranking manipulated images high;
- and the overall reliability of the method at different ELA quality levels.

Chapter 5

Results

The ranking results gathered from the experiments discussed in chapter 4 are incorporated in the graphs below. Each graph represents a different level of quality that was used for ELA. Figure 5.1 illustrates the ranking results for a quality of 75%, figure 5.2 for 85%, and figure 5.3 for 95%. Furthermore, the X-axis (horizontal axis) contains the images that were ranked. As described in chapter 4, a set of 300 images were used during the experiment, of which a total of 30 images were manipulated. The Y-axis (vertical axis) contains the 30 manipulated image as a different set in percentage.

For example in figure 5.1 using method 4, the number 40 on the X-axis indicates that out of the 40 images in the ranked results (probability of manipulation from high to low), a total of 20% of the manipulated images are included in these ranking results. Obviously, at number 300 on the X-axis, 100% of the manipulated images have been ranked.

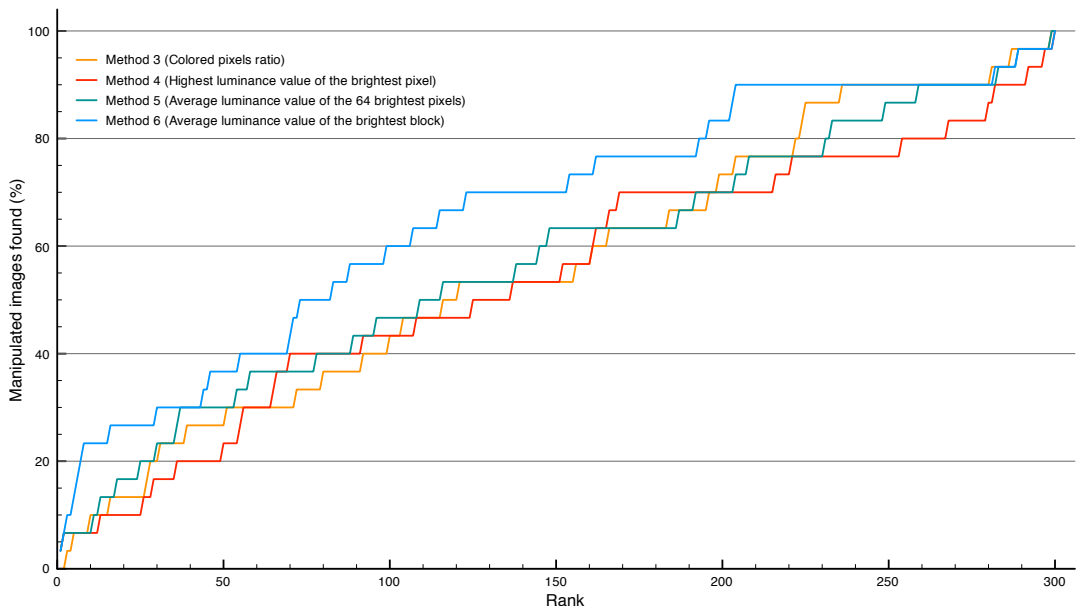


Figure 5.1: Ranking methods at 75% quality

The results illustrated in figure 5.1 show that at a quality level of 75%, method 6 yields the best results in ranking manipulated images when compared to the other three methods. The results produced by these three methods are similar to one another. However up until the 165 images that are ranked highest, method 5 is more consistent in ranking manipulated image higher.

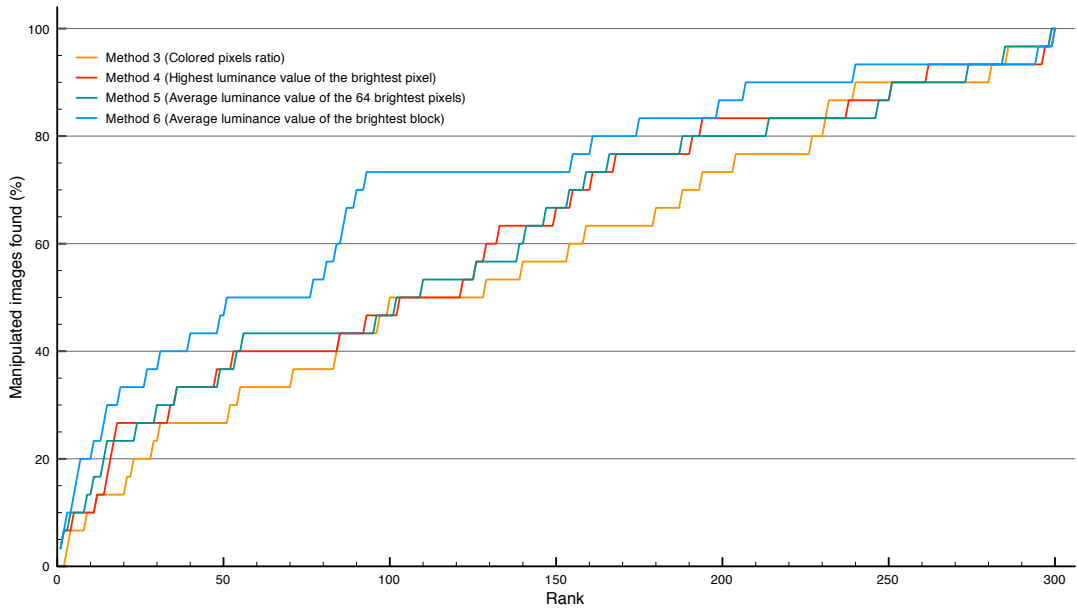


Figure 5.2: Ranking methods at 85% quality

The results illustrated in figure 5.2 show that at a quality level of 85%, method 6 again yields the best results in ranking manipulated images when compared to the other three methods. The results produced by method 3 are the worst. The other methods, 4 and 5, have very similar results.

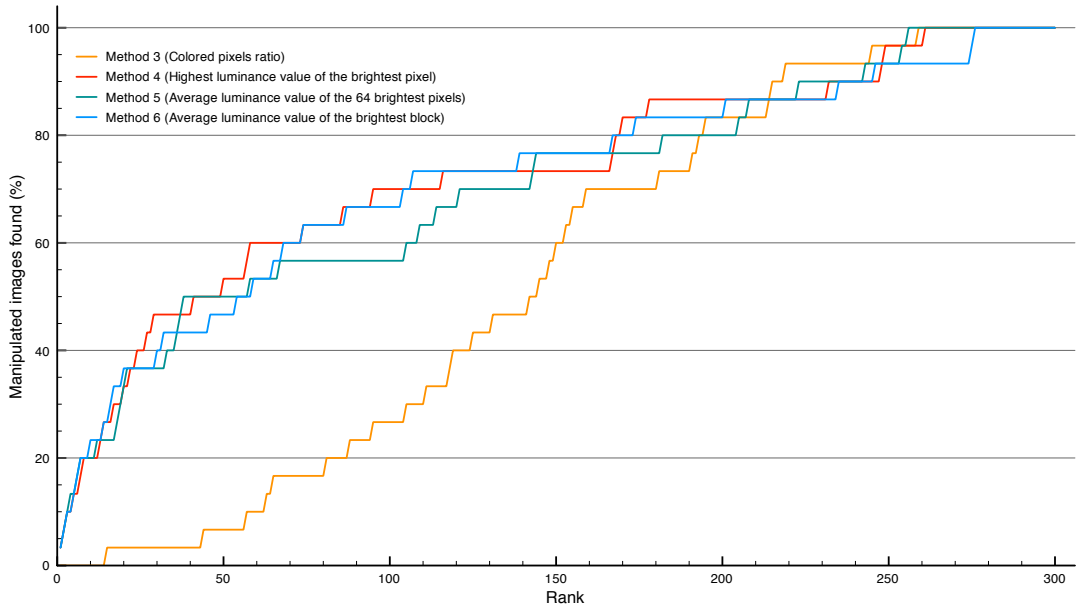


Figure 5.3: Ranking methods at 95% quality

Lastly, the results illustrated in figure 5.3 show that at a quality level of 95%, all methods perform similar with the exception of method 3 which by far produces the worst results.

When comparing the figures to each other, one can easily tell that figure 5.3 yields the best results in ranking 75% of the images that are manipulated in the first half of the ranking.

An in depth discussion of the results follows in chapter 6.

Chapter 6

Discussion

An observation of the results produced by each method at different quality levels was given in chapter 5 using graphs. The results in these graphs illustrate that for the set of 300 images $\{1, 2, 3, \dots, 298, 299, 300\}$ used for the experiment, 30 of these images, identified by <number>-M, are randomly manipulated by a third-party, and that the best results are achieved at an ELA quality level of 95%.

These graphs also illustrate that at a quality level of 75% and 85% there is not a lot of difference between the results of each method. At a quality level of 95%, however, method 3 shows different behavior compared to the other methods and a significant decline in the top 50 ranking results. This could be the result of the vast amount of black pixels present in the ELA results at a quality level of 95%, and with many authentic images still showing more noise compared to manipulated images.

Tables C, C.2 and C.3 show that two images, '015-M' and '228-M', are prominently at the top of the ranking at every quality level for methods 4, 5 and 6. The ELA results of images '015-M' and '228-M', illustrated in figures 6.1 to 6.6, clearly show a distortion in the noise pattern indicating manipulations being present.



Figure 6.1: 015-M - ELA performed at 75%



Figure 6.2: 015-M - ELA performed at 85%

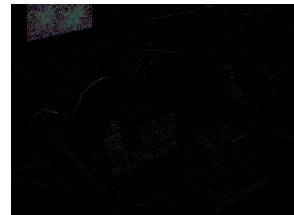


Figure 6.3: 015-M - ELA performed at 95%



Figure 6.4: 228-M - ELA performed at 75%



Figure 6.5: 228-M - ELA performed at 85%



Figure 6.6: 228-M - ELA performed at 95%

Looking at the corresponding original and manipulated images of '015-M' and '228-M', figures B.5, B.6, B.49, and B.50, we can indeed see the manipulations done and that they correspond to the noise patterns in the ELA results. The manipulations done in these two images, according to table A.1, are added JPEG images, something ELA is particularly effective at. However, according to the same table, images '002-M', '112-M', and '192-M' have added JPEG pictures as well but do not show up as high in the ranking.

Figures 6.7 to 6.9 show the ELA results for image '002-M'. The results at 75% and 85% show the bottle-cap and the batteries as potential manipulations, however, according to table A.1 only the bottle-cap has been added to the image. This manipulation is only distinguishable in the ELA result at a quality level of 95% but the image still does not show up in any of the rankings performed at a 95% quality level. For methods 4, 5 and 6 this could be explained by that the luminance value of the noise itself, whether calculated for pixels or blocks, is rather low compared to other results that appear higher in the ranking. Furthermore, the manipulated area is rather small which may in turn explain why it does not show up in the top 10 ranking for method 1.



Figure 6.7: 002-M - ELA performed at 75%



Figure 6.8: 002-M - ELA performed at 85%



Figure 6.9: 002-M - ELA performed at 95%

The ELA results for images '112-M' and '192-M', illustrated in figures 6.10 to 6.15, show no clear signs of manipulations even though table A.1 states that JPEG images have been added. Comparing the original images in figures B.23, B.39, and the manipulated images in figures B.24, B.40, we can clearly see the manipulations, which unfortunately, do not show up in the ELA results. An explanation for this could be that the added JPEG images have the same quality levels as the original images, therefore resulting in hardly any noise.

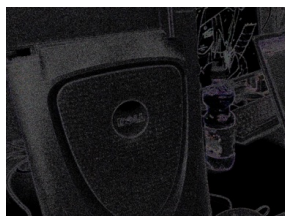


Figure 6.10: 112-M - ELA performed at 75%

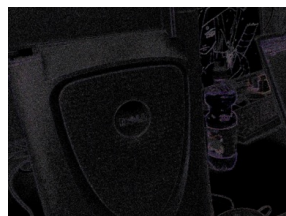


Figure 6.11: 112-M - ELA performed at 85%

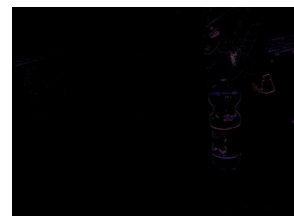


Figure 6.12: 112-M - ELA performed at 95%



Figure 6.13: 192-M - ELA performed at 75%



Figure 6.14: 192-M - ELA performed at 85%



Figure 6.15: 192-M - ELA performed at 95%

Image '281' has not been manipulated and still shows up in the top 10 ranking for methods 3, 4 and 5 at a quality level of 75% and 85%. Interestingly enough, this image is not in the top 10 rankings for any of the methods at a quality level of 95%. Figures 6.16 and 6.17 illustrate a very bright noise pattern which may explain why the image is ranked so high in methods 3, 4 and 5. However, at a 95% quality level, illustrated in figure 6.18, the image shows hardly any noise and therefore is not showing up in the top 10 rankings at a 95% quality level.



Figure 6.16: 281 - ELA performed at 75% Figure 6.17: 281 - ELA performed at 85% Figure 6.18: 281 - ELA performed at 95%

Two other non-manipulated images that show up in the top 10 rankings are '299' and '066'. Figures 6.19 to 6.24 illustrate a lot of noise present at every quality level. Comparing these ELA results to the results of image '281' in figures 6.16 to 6.18, it shows that all three images start off with noticeable patterns of noise at 75% and 85%, but only images '229' and '066' show noticeable patterns of noise at 95%. This explains why these two images do show up in the 95% quality rankings as where image '281' does not. This is probably due to a limitation of ELA, mentioned in section 2.4.1, where the noise in the ELA result is directly affected by the coloring and brightness of the original picture.



Figure 6.19: 299 - ELA performed at 75% Figure 6.20: 299 - ELA performed at 85% Figure 6.21: 299 - ELA performed at 95%

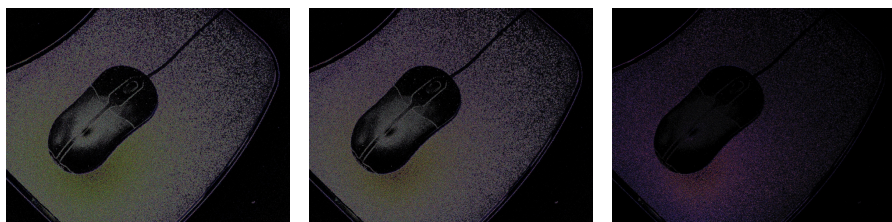


Figure 6.22: 066 - ELA performed at 75% Figure 6.23: 066 - ELA performed at 85% Figure 6.24: 066 - ELA performed at 95%

Figures, B.41 and B.42 show a subtle internal copy & move manipulation of the word 'tea', which is the only made manipulation according to table A.1. Unfortunately, the ELA results illustrated in figures 6.25 to 6.27 show no clear signs of the manipulation and yet the image is ranked in the top 10 for methods 4, 5 and 6 at a quality level of 95%.

So even though the image has been manipulated, the areas of the image that have been used as the qualifier are most likely not the areas that have been manipulated. Therefore, this image can be classified as a false positive.



Figure 6.25: 194-M - Figure 6.26: 194-M - Figure 6.27: 194-M -
ELA performed at 75% ELA performed at 85% ELA performed at 95%

Instead of looking at the top 10 rankings, we can take a look at the lowest 10 rankings for each method at each of the previously used levels of quality. Appendix D shows the tables with the images that have been ranked lowest.

It is interesting to see that at an ELA quality level of 95% no manipulated images are present in the lowest 10 rankings. However, at quality levels of 75% and 85% quite some manipulated images have been ranked in the lowest 10 rankings.

One image that scores particularly low is image '266-M'. Table A.1 states that the manipulation done to the picture is an internal copy & move manipulation of the upper part of the drawing which can be confirmed by looking at figures B.59 and B.60. The corresponding ELA results are illustrated in figures 6.28 to 6.30 and hardly show any noise at all, let alone noise that can identify the manipulation. There being almost no noise at any quality level is probably a side effect of one of the limitations in ELA and also explains why this image is ranked so low.



Figure 6.28: 266-M - Figure 6.29: 266-M - Figure 6.30: 266-M -
ELA performed at 75% ELA performed at 85% ELA performed at 95%

Image '178-M' scores very low as well. Figures B.35 and B.36 illustrate once again subtle internal copy & move manipulations. Once again, the ELA results illustrated in figures 6.31 to 6.33, show no clear signs of the manipulations.

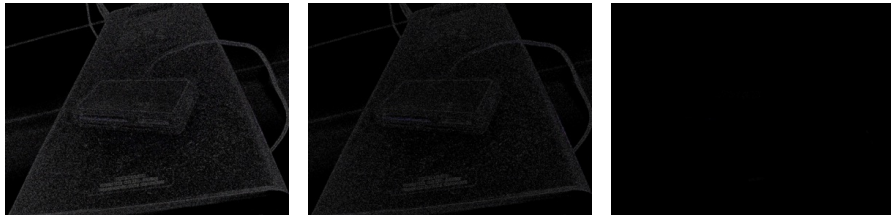


Figure 6.31: 178-M - Figure 6.32: 178-M - Figure 6.33: 178-M -
ELA performed at 75% ELA performed at 85% ELA performed at 95%

For a quality level of 75%, image '256-M' is ranked low. However, table A.1 tells us that this image has not been manipulated. One could argue that the result of ELA at a quality level of 75%, illustrated in figure 6.34, could be interpreted as if a manipulation is present, however, the ELA results at quality levels of 85% and 95% dispel this argument. The ranking position of this image is therefore a very valid one.



Figure 6.34: 256-M - Figure 6.35: 256-M - Figure 6.36: 256-M -
ELA performed at 75% ELA performed at 85% ELA performed at 95%

The manipulated images that have been ranked in the lowest 10 all have something in common, namely that the manipulations that have been performed are internal copy & move manipulations. Table A.1 tells us that there are more images on which internal copy & move manipulations have been performed. Appendix E, figures E.1 to E.3, illustrate the ranking for these manipulated images for each method at the different quality levels. Interesting to see is that most of the internal copy & move manipulated images are ranked relatively low at 75% quality but get a better ranking the more the quality increases. Three of these images rank very high, namely '108-M', '176-M' and '194-M'. The reason why image '194-M' is ranked so high has already been discussed. The ELA results for images '108-M' and '176-M' are illustrated in figures 6.37 to 6.40 and show the same particularities as image '194-M'. Therefore the same reasoning applies as to why these two images rank so high as well. It is therefore relatively safe to say that images that have been manipulated using the internal copy & move technique, do not show any signs of manipulation in their ELA results and therefore get ranked low.

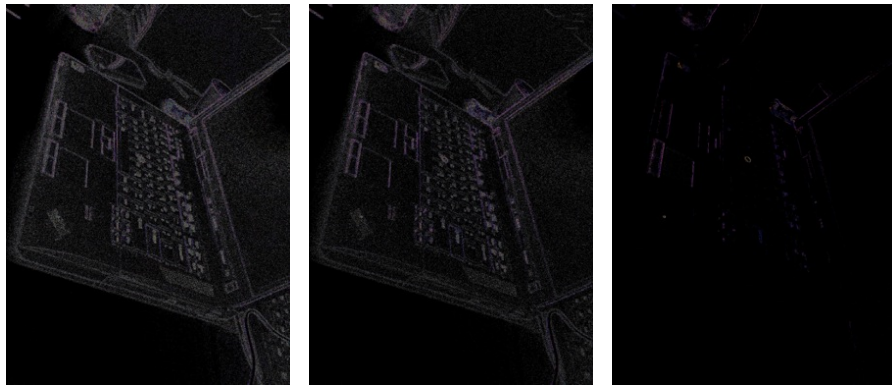


Figure 6.37: 108-M - Figure 6.38: 108-M - Figure 6.39: 108-M -
ELA performed at 75% ELA performed at 85% ELA performed at 95%



Figure 6.40: 176-M - Figure 6.41: 176-M - Figure 6.42: 176-M -
ELA performed at 75% ELA performed at 85% ELA performed at 95%

So far only images that have been manipulated by adding a JPEG image have shown very clear ELA results. And even amongst these images, not all rankings were very high. It also became clear that images with internal copy & move manipulations rank very low. Therefore, it is interesting to look at the images that have been manipulated using different types of techniques. Table A.1 shows that images '061-M', '071-M', '186-M', and '249-M' have been manipulated by adding text to the image. When we take a look at the ELA results of one of these images, in this case image '249-M', we can see that in the ELA results at quality levels of 75% and 85%, illustrated in figures 6.43 and 6.44, the manipulation is clearly visible. However, this image is ranked close to the middle of the ranking scale. This seems odd as the manipulation is so clearly present. A reason for it looking so bright could be because the rest of the image has hardly any noise, making it only appear brighter than it actually is.



Figure 6.43: 249-M - Figure 6.44: 249-M - Figure 6.45: 249-M -
ELA performed at 75% ELA performed at 85% ELA performed at 95%

Chapter 7

Conclusion

Ranking results can be achieved by using a qualifier based on the calculations of the ratio of colored pixels, the highest luminance value of the brightest pixel, the average luminance value of the 64 brightest pixels, or the average luminance value of the brightest block. Respectively, the best ranking results can be achieved by using these methods at an ELA quality level of 95%. However, none of these methods is clearly better than the other. Too many false positives are ranked before actual manipulated images and too many manipulated images have been ranked using qualifiers not based on their manipulated areas.

The ELA algorithm can only be used to detect external copy & move image manipulation techniques, and even those techniques are not always detected. In contrast to what [12] shows, internal copy & move manipulations are not seen at all, reducing the detectable manipulation techniques even further. The limitations of the ELA algorithm also influence the patterns and brightness in their corresponding ELA results which in turn influences the result of our methods, resulting in the finding of false positives.

As it stands now, an expert would still need to manually verify each ranked image to determine if it is manipulated. Not enough certainty can be given that manipulated images get ranked higher than authentic images, and therefore the ranking will not help in aiding an expert by reducing the amount of work.

To conclude, ELA can be used to rank a set of images as we have shown during this research. By using our methods, the set of images can be sorted with some of the manipulated images on top. However, when all manipulated images need to be found in a set, an exhaustive search by inspecting each image manually still seems the only viable option.

Chapter 8

Further Research

The results and discussion in respectively chapters 5 and 6 have given insight in the areas where further research is required. Research could be done in using image manipulation detection techniques other than the ELA algorithm to be used as a basis for the ranking system. Using different techniques could potentially aid in improving the reliability of the final ranking results.

Furthermore, it might prove fruitful to investigate the possibility of combining the outcome of multiple rankings. One could perform rankings at different ELA quality levels and combine these rankings in an attempt to have more effective and reliable results.

Not only can different rankings based on ELA be combined, it might also yield positive results by ranking based on different ranking methods and finally combining the outcome of these different rankings.

Finally, it might be possible for someone to develop a different ranking method that can determine a more reliable qualifier for the ranking system.

Acronyms

ELA Error Level Analysis

JPEG Joint Photographic Experts Group

GIF Graphics Interchange Format

PNG Portable Network Graphics

TIFF Tagged Image File Format

EXIF Exchangeable Image File Format

PCA Principal Component Analysis

WT Wavelet Transformations

LG Luminance Gradient

CG Computer Generated

DCT Discrete Cosine Transformation

PC Principal Component

Acknowledgements

We, Daan Wagenaar and Jeffrey Bosma, are grateful to the following people for their insight, suggestions, feedback, and (technical) opinions: Zeno Geraads (Netherlands Forensic Institute), Marcel Worring (University of Amsterdam), and Paolo Grosso (University of Amsterdam).

A special thanks goes out to Joas Wagenaar, in this document referred to as third-party, for creating some manipulated images with very realistic and indistinguishable manipulations.

Bibliography

- [1] S. Preston, “The science behind the red-eye effect,” March 2011. <http://www.cameratechnica.com/2011/03/14/the-science-behind-the-red-eye-effect/>.
- [2] M. Zimba and S. Xingming, “Dwt-pca (evd) based copy-move image forgery detection,” tech. rep., The School of Computer and Communications, Hunan University, January 2011.
- [3] T. Shahid and A. B. Mansoor, “Copy-move forgery detection algorithm for digital images and a new accuracy metric,” tech. rep., College of Aeronautical Engineering, National University of Sciences and Technology, November 2009.
- [4] “The commissar vanishes,” September 1999. http://www.newseum.org/berlinwall/commissar_vanishes/vanishes.htm.
- [5] D. Lucas, “Katie couric’s weight loss,” 2006. http://www.famouspictures.org/mag/index.php?title=Altered_Images#Katie_Couric.27s_weight_loss_-_2006.
- [6] CompuServe, “Graphics interchange format(sm),” tech. rep., PNG Development Group, 1999.
- [7] M. Adler, T. Boutell, and J. Bowler, “Png (portable network graphics) specification, version 1.0,” tech. rep., CompuServe Incorporated, 1990.
- [8] A. D. Association, “Tiff revision 6.0,” tech. rep., Adobe, June 1992.
- [9] M. Reichmann, “Understanding raw files explained.” <http://www.luminous-landscape.com/tutorials/understanding-series/u-raw-files.shtml>.
- [10] “Exchangeable image file format for digital still cameras: Exif version 2.2,” tech. rep., Japan Electronics and Information Technology Industries Association, April 2002.
- [11] R. Tortorella, “Image doctoring: Jpeg encoding and analysis,” tech. rep., National Aviation Reporting Center on Anomalous Phenomena, May 2009.
- [12] N. Krawetz, “A picture’s worth, digital image analysis,” tech. rep., 2007.
- [13] “Detecting image forgery - state of the art,” March 2009.
- [14] L. I. Smith, “A tutorial on principal components analysis,” tech. rep., University of Otago, February 2002.
- [15] D. Santa-Cruz and T. Ebrahimi, “An analytical study of jpeg 2000 functionalities,” tech. rep., Swiss Federal Institute of Technology, September 2000.
- [16] J. Miano, *Compressed Image File Formats JPEG, PNG, GIF, XBM, BMP*. ACM Press, July 2009.
- [17] M.-Y. Shen and C.-C. J. Kuo, “Review of postprocessing techniques for compression artifact removal,” tech. rep., March 1998.
- [18] D. Austin, “Image compression: Seeing what’s not there.” <http://www.ams.org/samplings/feature-column/fcarc-image-compression>.

- [19] S. A. Khayam, "The discrete cosine transform (dct): Theory and application," tech. rep., Department of Electrical & Computer Engineering, Michigan State University, March 2003.
- [20] N. Krawetz, "Resaving images," February 2010. <http://www.hackerfactor.com/blog/index.php?/archives/354-Resaving-Images.html>.
- [21] D. R. Finley, "Hsp color model - alternative to hsv (hsb) and hsl," 2006. <http://alienryderflex.com/hsp.html>.
- [22] K. R. Spring, T. J. Fellers, and M. W. Davidson, "Human vision and color perception," tech. rep., Florida State University, August 2003.

Appendix A

Overview of Performed Manipulations

Image	Copy & Move (C&M) Image Manipulation(s)
002-M	External C&M: added a JPEG image of a bottle cap.
013-M	Internal C&M: added the red wall plugs.
015-M	External C&M: added a JPEG image of a painting.
050-M	Internal C&M: added a Post-it note pad.
061-M	External C&M: added Computer Generated (CG) text onto the wall.
071-M	Internal C&M: added the stickers on the TV, and added CG text onto the cardboard box.
081-M	Internal C&M: removed the icons above the buttons of the LCD monitor.
083-M	Internal C&M: modified (rotated) the numbers on the red sticker on the phone, and an internal C&M to remove the text from a button of the phone.
093-M	Internal C&M: added a part of the instructions.
099-M	Internal C&M: modified the label of one of the batteries.
108-M	Internal C&M: added a second touch pad to the notebook.
112-M	External C&M: added a JPEG image onto the LCD monitor.
125-M	Internal C&M: removed a screw from the device casing.
129-M	Internal C&M: added parts to the painting.
146-M	Internal C&M: removed lining from the wall.
157-M	Internal C&M: removed the cloth.
176-M	Internal C&M: removed parts of the computer casing, and an internal copy & paste of a sticker.
178-M	Internal C&M: removed the logo from the device casing, and an internal C&M to remove the computer's serial number.
186-M	External C&M: added an image to the cardboard box.
192-M	External C&M: added a JPEG image of an apple.
194-M	Internal C&M: added text.
196-M	Internal C&M: added a screw in the power socket.
197-M	Internal C&M: modified parts of the Post-it note pad.
208-M	Internal C&M: modified parts of the text on the display of the heartbeat monitor.
228-M	External C&M: added a JPEG image of a mobile phone.
247-M	Internal C&M: removed a device.
249-M	External C&M: added CG text onto the paper in the flatbed scanner.
254-M	Internal C&M: modified the text on the label.
256-M	No manipulations were performed.
266-M	Internal C&M: added a part to the drawing.

Table A.1: Performed manipulations

Appendix B

Overview of Manipulated Images

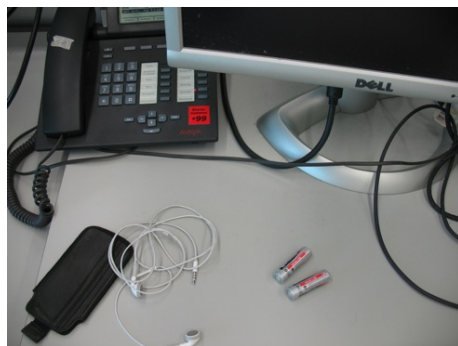


Figure B.1: 002 - Original

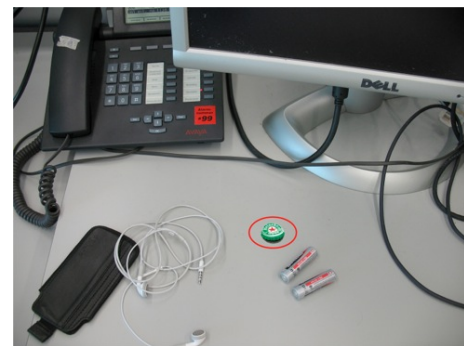


Figure B.2: 002 - Manipulated



Figure B.3: 013 - Original

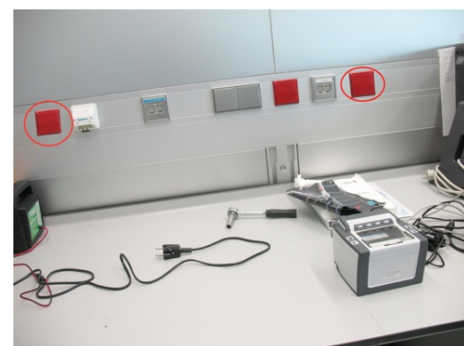


Figure B.4: 013 - Manipulated



Figure B.5: 015 - Original



Figure B.6: 015 - Manipulated



Figure B.7: 050 - Original



Figure B.8: 050 - Manipulated



Figure B.9: 061 - Original



Figure B.10: 061 - Manipulated



Figure B.11: 071 - Original



Figure B.12: 071 - Manipulated



Figure B.13: 081 - Original



Figure B.14: 081 - Manipulated



Figure B.15: 083 - Original



Figure B.16: 083 - Manipulated



Figure B.17: 093 - Original



Figure B.18: 093 - Manipulated

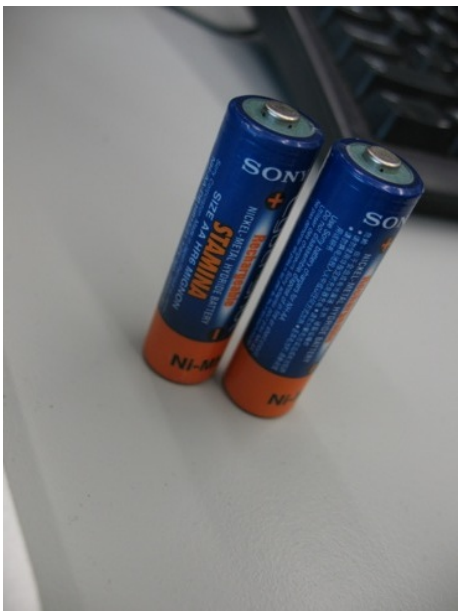


Figure B.19: 099 - Original



Figure B.20: 099 - Manipulated



Figure B.21: 108 - Original

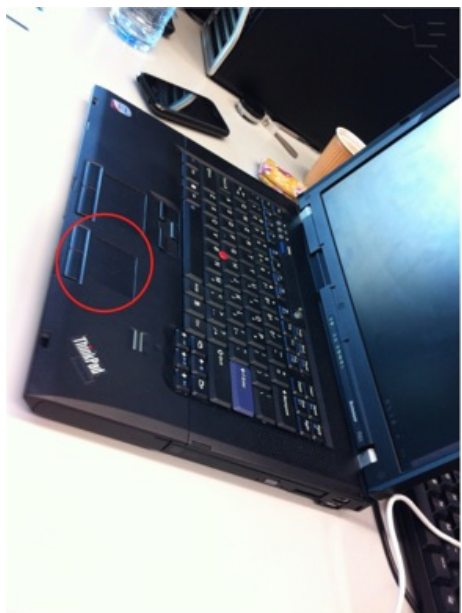


Figure B.22: 108 - Manipulated



Figure B.23: 112 - Original



Figure B.24: 112 - Manipulated



Figure B.25: 125 - Original



Figure B.26: 125 - Manipulated



Figure B.27: 129 - Original



Figure B.28: 129 - Manipulated



Figure B.29: 146 - Original



Figure B.30: 146 - Manipulated



Figure B.31: 157 - Original



Figure B.32: 157 - Manipulated



Figure B.33: 176 - Original



Figure B.34: 176 - Manipulated



Figure B.35: 178 - Original



Figure B.36: 178 - Manipulated



Figure B.37: 186 - Original



Figure B.38: 186 - Manipulated



Figure B.39: 192 - Original



Figure B.40: 192 - Manipulated



Figure B.41: 194 - Original



Figure B.42: 194 - Manipulated



Figure B.43: 196 - Original



Figure B.44: 196 - Manipulated



Figure B.45: 197 - Original

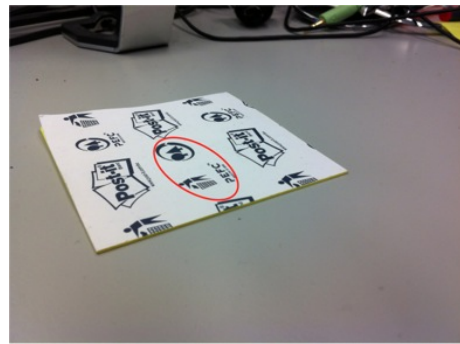


Figure B.46: 197 - Manipulated



Figure B.47: 208 - Original



Figure B.48: 208 - Manipulated



Figure B.49: 228 - Original



Figure B.50: 228 - Manipulated



Figure B.51: 247 - Original

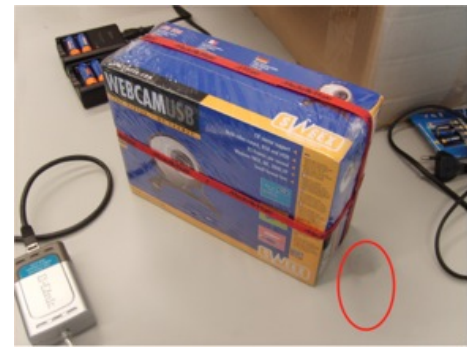


Figure B.52: 247 - Manipulated

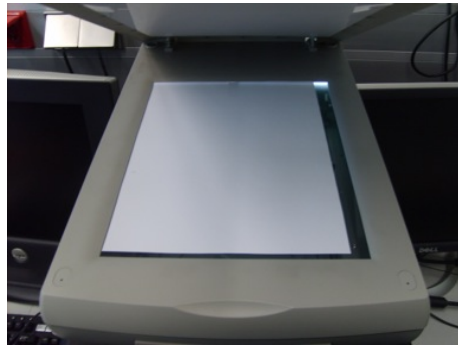


Figure B.53: 249 - Original



Figure B.54: 249 - Manipulated

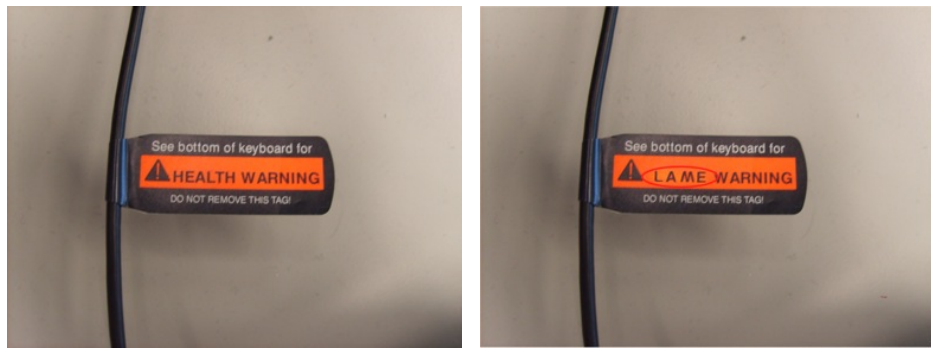


Figure B.55: 254 - Original

Figure B.56: 254 - Manipulated



Figure B.57: 256 - Original

Figure B.58: 256 - No change

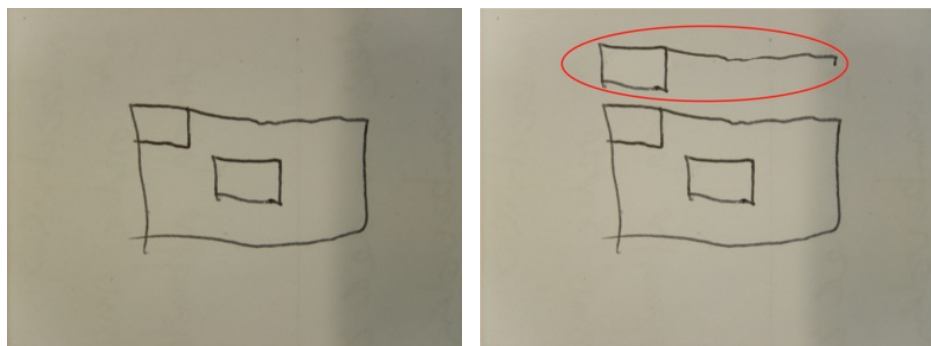


Figure B.59: 266 - Original

Figure B.60: 266 - Manipulated

Appendix C

Highest 10 Ranking Results

Rank	Method 3	Method 4	Method 5	Method 6
1	066	228-M	015-M	228-M
2	281	015-M	228-M	015-M
3	176-M	293	281	186-M
4	107	281	293	299
5	186-M	271	299	194-M
6	113	251	078	125-M
7	299	025	278	176-M
8	135	283	066	002-M
9	078	299	025	066
10	157-M	078	041	010

Table C.1: Highest 10 images at 75%

Rank	Method 3	Method 4	Method 5	Method 6
1	066	228-M	015-M	228-M
2	281	015-M	228-M	015-M
3	176-M	281	281	194-M
4	186-M	299	125-M	299
5	078	125-M	299	186-M
6	107	025	293	176-M
7	299	041	078	125-M
8	113	293	025	066
9	157-M	078	066	032
10	1 35	259	083-M	065

Table C.2: Highest 10 images at 85%

Rank	Method 3	Method 4	Method 5	Method 6
1	066	228-M	015-M	015-M
2	078	015-M	228-M	228-M
3	299	125-M	125-M	194-M
4	028	066	066	299
5	029	108-M	194-M	176-M
6	293	054	176-M	186-M
7	051	194-M	108-M	125-M
8	271	176-M	032	032
9	025	032	011	066
10	090	011	054	254-M

Table C.3: Highest 10 images at 95%

Appendix D

Lowest 10 Ranking Results

Rank	Method 3	Method 4	Method 5	Method 6
291	277	168	232	131
292	239	178-M	235	023
293	209	105	256-M	232
294	221	172	195	172
295	234	264	163	240
296	246	195	234	127
297	287	256-M	206	163
298	284	142	142	264
299	266-M	206	264	142
300	295	266-M	266-M	266-M

Table D.1: Lowest 10 images at 75%

Rank	Method 3	Method 4	Method 5	Method 6
291	209	163	130	286
292	221	168	131	232
293	239	130	127	173
294	277	127	137	284
295	246	280	234	178-M
296	284	142	163	142
297	234	178-M	104	163
298	287	137	142	264
299	266-M	104	266-M	131
300	295	266-M	264	266-M

Table D.2: Lowest 10 images at 85%

Rank	Method 3	Method 4	Method 5	Method 6
291	136	115	136	136
292	180	168	195	180
293	115	166	115	163
294	166	171	166	131
295	131	136	131	184
296	184	172	127	168
297	127	195	163	166
298	163	160	184	160
299	160	131	168	127
300	168	184	160	115

Table D.3: Lowest 10 images at 95%

Appendix E

Ranking of Internal Copy & Move Manipulated Images

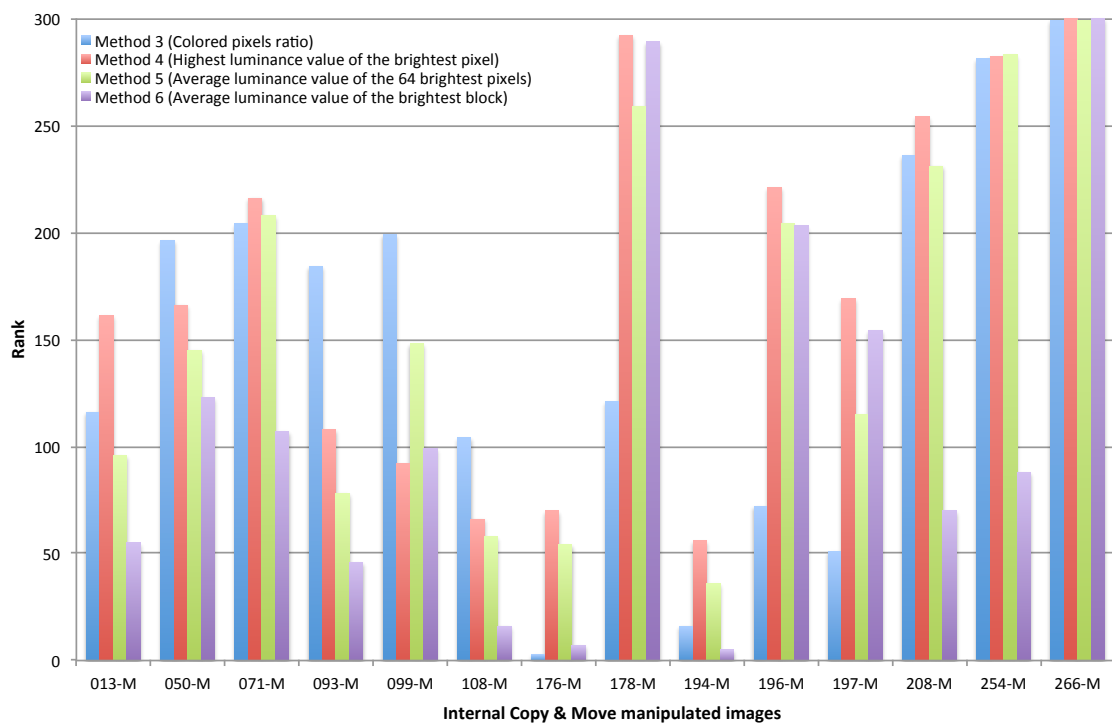


Figure E.1: Ranking of internal copy & move manipulated images at 75% (lower is better)

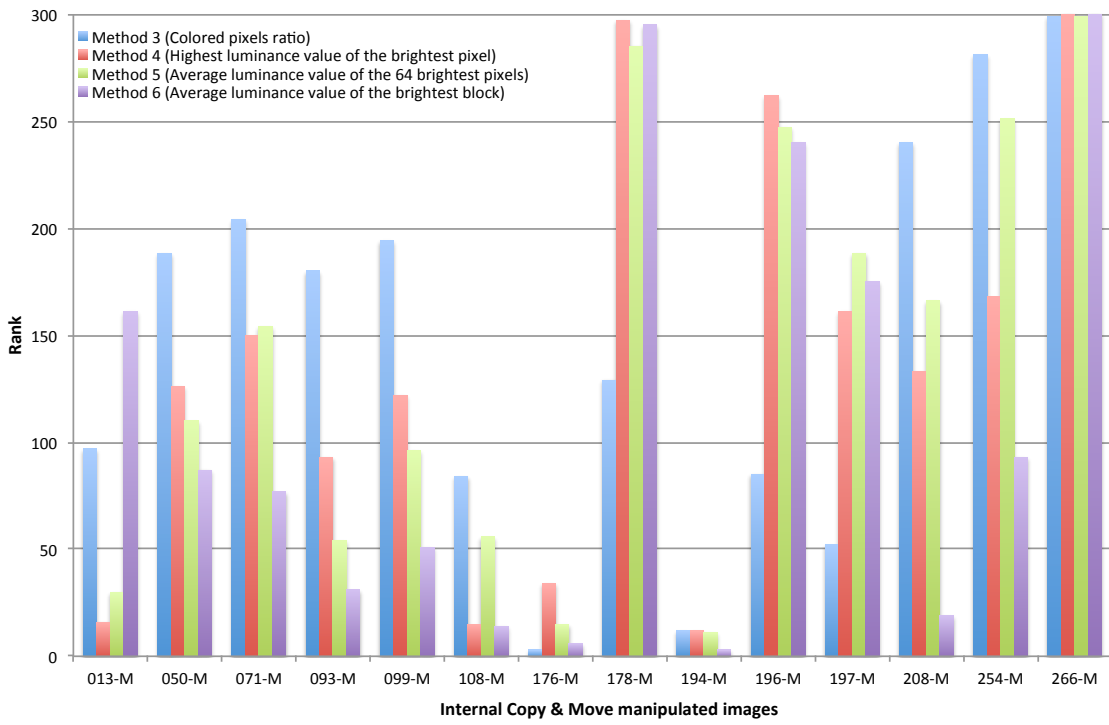


Figure E.2: Ranking of internal copy & move manipulated images at 85% (lower is better)

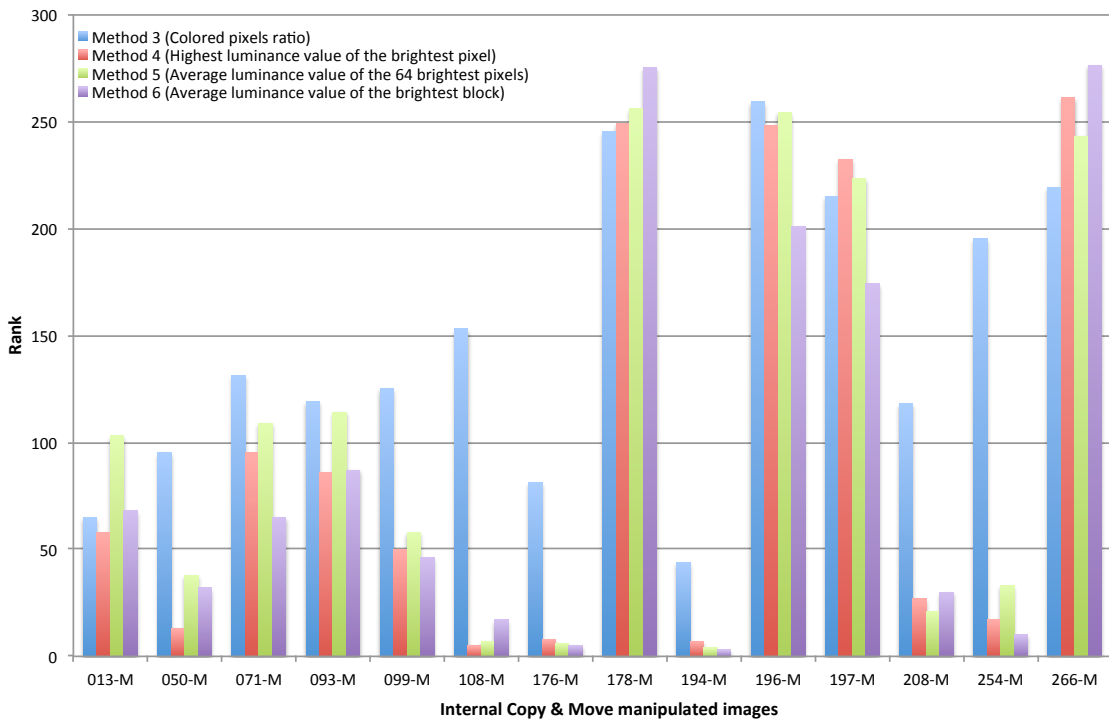


Figure E.3: Ranking of internal copy & move manipulated images at 95% (lower is better)